Inorg. Chem. **2009**, *48*, 646−651

Tetra- and Decanuclear Iron(III) Phosphonates: Observance of a Rare P−C Bond Cleavage in a Homogeneous Medium

Ramaswamy Murugavel,*,†,‡ Nayanmoni Gogoi,† and Rodolphe Clérac§,⊥

Department of Chemistry and Centre for Research in Nanotechnology and Science (CRNTS), Indian Institute of Technology−Bombay, Powai, Mumbai-400076, India, and CNRS, UPR 8641, Centre de Recherche Paul Pascal (CRPP), Equipe "Matériaux Moléculaires Magnétiques", 115 avenue du Dr. Albert Schweitzer, Pessac, F-33600, France, and Université de Bordeaux, UPR 8641, Pessac, F-33600, France

Received September 12, 2008

Reactions of *tert*-butylphosphonic acid (^{t}BuPO$_3$H$_2$) with two different Fe(III) precursors have been investigated. The reaction of precursor complex [Fe$_3$(μ_3-O)(O$_2$CPh)$_6$(H$_2$O)$_3$]Cl with ^{t}BuPO$_3$H$_2$ in pyridine (py) leads to the formation of tetranuclear iron(III)phosphonate [Fe$_4$O(^{t}BuPO$_3$)$_3$(O$_2$CPh)$_3$(py)$_3$Cl]·3.5py (**1**) as single crystals. The change of the Fe(III) source to FeCl$_3$ under similar reaction conditions results in the isolation of decanuclear complex [Fe$_{10}$(OH)$_8$(HPO$_4$)(^{t}BuPO$_3$)$_8$(^{t}BuPO$_3$H)$_4$(py)$_8$]·4py·5H$_2$O (**2**). Compounds **1** and **2** have been characterized by elemental analysis, spectroscopic studies, and single-crystal X-ray diffraction studies. While the structure of **1** could be described as a tetrahedral cluster supported by benzoate and phosphonate ligands, the molecular structure of **2** is unprecedented in metal phosphonate chemistry. In the course of formation of **2**, ^{t}BuPO$_3$H$_2$ undergoes a rare P−C bond cleavage at room temperature and produces the phosphate anion, which then acts as a template for the construction of a novel decanuclear iron−phosphate−phosphonate with a hitherto unknown core architecture. The temperature dependence of the χT product in **2** reveals dominant antiferromagnetic interactions between Fe(III) centers.

Introduction

There has been considerable interest in the use of main group compounds containing many acidic hydrogen atoms (e.g., hydroxyl, amino, and acid groups) to build cagelike molecules, extended polymers, and three-dimensional framework solids including metal-organic frameworks. Polycarboxylic acids, organosilanetriols, and phosphonic/phosphoric acids have been extensively used for this purpose in the past decade.[1] We have been particularly interested in a room-temperature building-block approach for the rational synthesis of cagelike and zeolite-like metal phosphonate or phosphate materials.[2−4] In this endeavor, after having incorporated main group elements in the zeolite SBU look-

* Author to whom correspondence should be addressed. Fax: +91-22-2572 3480. E-mail: rmv@chem.iitb.ac.in.
† Department of Chemistry. IIT−Bombay.
‡ CRNTS, IIT−Bombay.
§ CNRS, UPR8641 CRPP.
⊥ Université de Bordeaux.

(1) (a) Murugavel, R.; Choudhury, A.; Pothiraja, R.; Walawalkar, M. G.; Rao, C. N. R. *Chem. Rev.* **2008**, *108*, 3549. (b) Murugavel, R.; Voigt, A.; Walawalkar, M. G.; Roesky, H. W. *Chem. Rev.* **1996**, *96*, 2205. (c) Rao, C. N. R.; Natarajan, S.; Vaidhyanathan, R. *Angew. Chem., Int. Ed.* **2004**, *43*, 1466. (d) Murugavel, R.; Davis, P.; Shete, V. S. *Inorg. Chem.* **2003**, *42*, 4696.

(2) (a) Murugavel, R.; Walawalkar, M. G.; Dan, M.; Roesky, H. W.; Rao, C. N. R. *Acc. Chem. Res.* **2004**, *37*, 763. (b) Walawalkar, M. G.; Roesky, H. W.; Murugavel, R. *Acc. Chem. Res.* **2001**, *32*, 201.

(3) (a) Murugavel, R.; Kuppuswamy, S.; Boomishankar, R.; Steiner, A. *Angew. Chem., Int. Ed.* **2006**, *45*, 5536. (b) Murugavel, R.; Kuppuswamy, S. *Angew. Chem., Int. Ed.* **2006**, *45*, 7022. (c) Murugavel, R.; Kuppuswamy, S. *Chem.—Eur. J.* **2008**, *14*, 3869. (d) Murugavel, R.; Kuppuswamy, S.; Randoll, S. *Inorg. Chem.* **2008**, *47*, 6028. (e) Murugavel, R.; Kuppuswamy, S. *Inorg. Chem.* **2008**, *47*, 7686. (f) Murugavel, R.; Shanmugan, S.; Kuppuswamy, S. *Eur. J. Inorg. Chem.* **2008**, 1508. (g) Murugavel, R.; Shanmugan, S. *Organometallics* **2008**, *27*, 2784. (h) Murugavel, R.; Shanmugan, S. *Chem. Commun.* **2007**, 1257. (i) Murugavel, R.; Shanmugan, S. *Dalton Trans.* **2008**, 5358.

(4) (a) Pothiraja, R.; Sathiyendiran, M.; Butcher, R. J.; Murugavel, R. *Inorg. Chem.* **2005**, *44*, 6314. (b) Pothiraja, R.; Sathiyendiran, M.; Butcher, R. J.; Murugavel, R. *Inorg. Chem.* **2004**, *43*, 7585. (c) Murugavel, R.; Sathiyendiran, M.; Pothiraja, R.; Walawalkar, M. G.; Mallah, T.; Riviere, E. *Inorg. Chem.* **2004**, *43*, 945. (d) Sathiyendiran, M.; Murugavel, R. *Inorg. Chem.* **2002**, *41*, 6404. (e) Murugavel, R.; Sathiyendiran, M. *Chem. Lett.* **2001**, 84. (f) Murugavel, R.; Sathiyendiran, M.; Walawalkar, M. G. *Inorg. Chem.* **2001**, *40*, 427. (g) Murugavel, R.; Pothiraja, R.; Gogoi, N.; Clérac, R.; Lecren, L.; Butcher, R. J.; Nethaji, M. *Dalton Trans.* **2007**, 2405. (h) Pothiraja, R.; Shanmugan, S.; Walawalkar, M. G.; Butcher, R. J.; Nethaji, M.; Murugavel, R. *Eur. J. Inorg. Chem.* **2008**, 1834. (i) Murugavel, R.; Sathiyendiran, M.; Pothiraja, R.; Butcher, R. J. *Chem. Commun.* **2003**, 2546.

10.1021/ic8017562 CCC: $40.75
Published on Web 12/16/2008

alike organic soluble metal phosphonate or phosphate complexes, we have turned our attention to transition metal ions, choosing Fe(III) as the example, with the additional objective that the new iron complexes apart from modeling SBUs of zeolites could also exhibit interesting magnetic properties.[5−7]

Since organophosphonate ligands can embrace many metal centers (up to six!), they have been extensively used to synthesize polynuclear complexes,[8] including a number of iron(III)−phosphonate cage complexes.[6,7] Interestingly, all polynuclear iron phosphonate compounds reported to date use trimeric precursors $[Fe_3O(O_2CR)_6(H_2O)_3]X$ (where X = Cl^-, NO_3^-, ClO_4^{2-}, etc.), as the starting point.[6] Iron phosphonate cage complexes obtained following this route contain both carboxylate and phosphonate ligands as the bridging unit but invariably retain the μ_3-oxo-centered trimeric $[Fe_3(\mu_3\text{-}O)]^{7+}$ unit in the product, except in the case of $[Fe_9(\mu\text{-}OH)_7(\mu\text{-}O)_2(O_3PC_6H_9)_8(py)_{12}]$.[7] We began our initial investigations with the reaction of phosphonic acid with triangular $[Fe_3(\mu_3\text{-}O)(O_2CR)_6(H_2O)_3]X$ precursors, but later used $FeCl_3 \cdot 6H_2O$, to prepare the first decanuclear Fe(III)−phosphonate complex. The results of this investigation, reporting a tetranuclear and an unusual decanuclear iron phosphonate, are described in this contribution.

Results and Discussion

Synthesis and Structure of Tetranuclear Phosphonate 1. The reaction between the Fe(III) precursor complex $[Fe_3(\mu_3\text{-}O)(PhCOO)_6(H_2O)_3]Cl$ and two equivalents of *tert*-butylphosphonic acid in pyridine leads to the formation of tetranuclear iron−phosphonate complex $[Fe_4O(^tBuPO_3)_3(O_2CPh)_3(py)_3Cl] \cdot 3.5py$ (**1**) (Scheme 1). The solid-state diffuse reflectance UV−visible spectrum of **1** shows absorption maxima at 493 and 415 nm. The infrared spectrum is typical of tetrameric iron phosphonates, with the bands for $\nu_{as}(COO)$ and $\nu_s(COO)$ appearing at 1602 and 1417 cm^{-1}, respectively. Bands at 1084, 1070, and 1005 cm^{-1} can be assigned for M−O−P and P═O stretching vibrations, while bands in the range 719−505 cm^{-1} are due to $\nu_{as}(Fe^{III}{}_3O)$.[6a−c]

Scheme 1. Synthesis of Compounds **1** and **2**

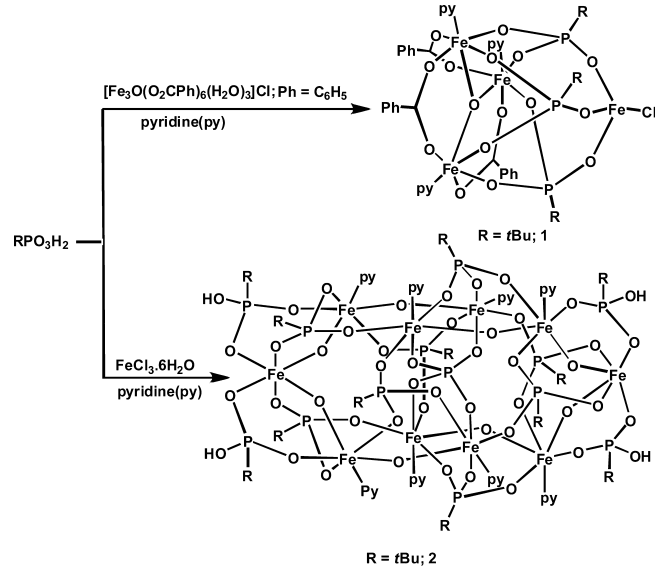

The most frequently observed structural types for tetranuclear iron complexes are either the butterfly-like arrangement[9a] or the cubane-like core.[9b] The four iron atoms in **1** form a tetrahedral cagelike structure (Figure 1), somewhat similar to those found in the cases of other tetranuclear iron phosphonates.[6a−c] The bottom of the tetranuclear cage consists of a μ_3-oxo-centered iron triangle similar to that of the starting material. The μ_3-O lies almost equidistant from octahedral Fe1, Fe2, and Fe3 ions (1.928(5),

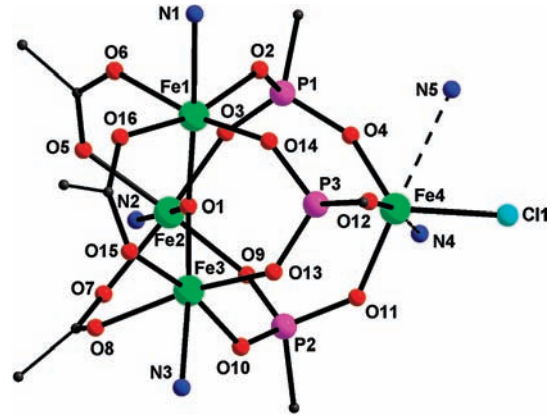

Figure 1. Core structure of **1**. N5 corresponds to a disordered pyridine with 0.5 occupancy. The other half interacts with the Fe4 of an adjacent molecule (see Figure 2). Selected bond lengths (Å) and bond angles: O(1)−Fe(1) 1.928(5), O(1)−Fe(2) 1.948(5), O(1)−Fe(3) 1.927(5), O(2)−Fe(1) 1.972(5), O(3)−Fe(2) 1.963(5), O(4)−Fe(4) 1.861(5), O(9)−Fe(2) 1.956(5), O(10)−Fe(3) 1.959(6), O(11)−Fe(4) 1.863(8), O(12)−Fe(4) 1.913(9), O(13)−Fe(3) 1.958(6), O(14)−Fe(1) 1.964(5), Cl(1)−Fe(4) 2.152(3), Fe(1)−N(1) 2.233(6), Fe(2)−N(2) 2.240(7), Fe(3)−N(3) 2.221(6), Fe(3)−O(1)−Fe(1) 120.7(3), Fe(3)−O(1)−Fe(2) 119.2(2), Fe(1)−O(1)−Fe(2) 119.6(2), O(14)−Fe(1)−O(2) 92.3(2), O(1)−Fe(2)−O(9) 97.1(2), O(1)−Fe(2)−O(3) 98.3(2), O(1)−Fe(3)−O(10) 95.5(2), O(4)−Fe(4)−O(11) 116.5(3), O(4)−Fe(4)−O(12) 106.1(3), O(11)−Fe(4)−O(12) 95.0(3), O(4)−Fe(4)−Cl(1) 119.96(19), O(11)−Fe(4)−Cl(1) 109.7(2).

(5) (a) Christou, G.; Gatteschi, D.; Hendrickson, D. N.; Sessoli, R. *MRS Bull.* **2000**, *25*, 66. (b) Gatteschi, D.; Sessoli, R.; Cornia, A. *Chem. Commun.* **2000**, 725. (c) Aromi, G.; Brechin, E. K. *Struct. Bonding (Berlin)* **2006**, *122*, 1.

(6) (a) Tolis, E. I.; Helliwell, M.; Langley, S.; Raftery, J.; Winpenny, R. E. P. *Angew. Chem., Int. Ed.* **2003**, *42*, 3804. (b) Konar, S.; Bhuvanesh, N.; Clearfield, A. *J. Am. Chem. Soc.* **2006**, *128*, 9604. (c) Yao, H. C.; Li, Y. Z.; Zheng, L. M.; Xin, X. Q. *Inorg. Chim. Acta* **2005**, *358*, 2523. (d) Tolis, E. I.; Engelhardt, L. P.; Mason, P. V.; Rajaraman, G.; Kindo, K.; Luban, M.; Matsuo, A.; Nojiri, H.; Raftery, J.; Schröder, C.; Timco, G. A.; Tuna, F.; Wernsdorfer, W.; Winpenny, R. E. P. *Chem.—Eur. J.* **2006**, *12*, 8961. (e) Konar, S.; Clearfield, A. *Inorg. Chem.* **2008**, *47*, 5573.

(7) Yao, H. C.; Wang, J. J.; Ma, Y. S.; Waldmann, O.; Du, W. X.; Song, Y.; Li, Y. Z.; Zheng, L. M.; Decurtins, S.; Xin, X. Q. *Chem. Commun.* **2006**, 1745.

(8) (a) Anantharaman, G.; Walawalkar, M. G.; Murugavel, R.; Gabor, B.; Herbst-Irmer, R.; Baldus, M.; Angerstein, B.; Roesky, H. W. *Angew. Chem., Int. Ed.* **2003**, *42*, 4482. (b) Chandrasekhar, V.; Kingsley, S. *Angew. Chem., Int. Ed.* **2000**, *39*, 2320. (c) Maheswaran, S.; Chastanet, G.; Teat, S. J.; Mallah, T.; Sessoli, R.; Wernsdorfer, W.; Winpenny, R. E. P. *Angew. Chem., Int. Ed.* **2005**, *44*, 5044. (d) Brechin, E. K.; Coxall, R. A.; Parkin, A.; Parsons, S.; Tasker, P. A.; Winpenny, R. E. P. *Angew. Chem., Int. Ed.* **2001**, *40*, 2700. (e) Walawalkar, M. G.; Horchler, S.; Dietrich, S.; Chakraborty, D.; Roesky, H. W.; Schäfer, M.; Schimdt, H.-G.; Sheldrick, G. M.; Murugavel, R. *Organometallics* **1998**, *17*, 2865.

(9) (a) Chaudhuri, P.; Rentschler, E.; Birkelbach, F.; Krebs, C.; Bill, E.; Weyhermuller, T.; Florke, U. *Eur. J. Inorg. Chem.* **2003**, 541. (b) Taft, K. L.; Caneschi, A.; Pence, L. E.; Delfs, C. D.; Papaefthymiou, G. C.; Lippard, S. J. *J. Am. Chem. Soc.* **1993**, *115*, 11753.

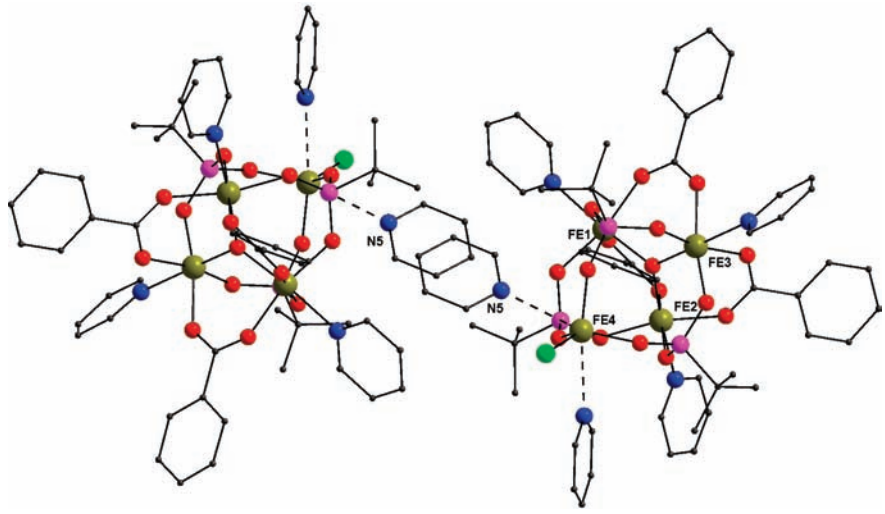

Figure 2. Disordered N5-pyridine bridges two adjacent tetramers **1** in crystal.

Table 1. Comparison of Structural Parameters of Tetrameric Iron Phosphonates

compound	Fe−O1(μ_3), Å	Fe−O(P), Å	Fe4−N(py), Å	reference
$[Fe_4O(tBuPO_3)_3(O_2CPh)_3(py)_3Cl]\cdot 3.5py$	1.927(5)−1.948(5)	1.861(5)−1.972(5)	2.666, 2.773	this work
$[Fe_4O(PhPO_3)_3\ (O_2CPh)_3(py)_5Cl]\cdot H_2O$	1.927−1.948	1.922−1.990	2.177, 2.291	6a
$[Fe_4O(C_{10}P)_3(O_2CCMe_3)_4(py)_4]\cdot 3CH_3CN$	1.928−1.961	1.896−1.992	2.211	6b
$[Fe_4O(C_6H_9PO_3)_3(O_2CMe)_3(py)_5Cl]\cdot 2H_2O$	1.928−1.936	1.949(2)−1.979(2)	2.193(3), 2.273(3)	6c

1.948(5), and 1.927(5) Å, respectively), and hence similar Fe···Fe distances (3.349, 3.342, and 3.350 Å) are observed.

Although the three phosphonate ligands within the μ_3-oxo-bridged trinuclear fragment in **1** function exactly as the benzoate ligand by bridging the adjacent metal ions, the additional oxygen on the phosphonate ligands is utilized to bridge the fourth Fe center (Fe4) via a [3.111] binding mode.[10] Thus, the tetrahedral Fe4 ion is surrounded by three phosphonate oxygen atoms and a chloride. Two very weak interactions with the nearby lattice pyridine molecules (Fe4···N4, 2.666 Å and Fe4···N5, 2.773 Å) have also been observed (Figures 1 and 2). In the cases of other tetrameric iron phosphonates, Fe4 adopts an octahedral geometry with the two pyridine molecules lying within the coordination sphere (Fe4−N distance, in $[Fe_4O(PhPO_3)_3(C_6H_5CO_2)_3(py)_5Cl]\cdot H_2O$,[6a] 2.177 and 2.291 Å and, in $[Fe_4O(C_6H_9PO_3)_3(O_2CMe)_3(py)_5Cl]\cdot 2H_2O$,[6c] 2.193(3) and 2.273(3) Å). Even in the case of $[Fe_4O(CamP)_3(O_2CCMe_3)_4(py)_4]$,[6b] [$H_2$CamP = camphyl phosphonic acid], the Fe4 atom attains a distorted octahedral geometry with the help of a terminal pyridine (Fe4−N 2.211 Å) and a chelating pivalate. Thus, the geometry found around Fe4 makes compound **1** unique among the tetrameric iron phosphonates (Table 1). One of the pyridine molecules (N5) coordinated to Fe4 is disordered with respect to the center of symmetry, and hence this pyridine bridges two adjacent molecules of **1** as shown in Figure 2.

Synthesis of Decanuclear Phosphonate 2. Since the reactions of triangular iron(III) starting materials invariably produce complexes with a central [$Fe_3(\mu_3$-O)] unit, we sought to use other Fe(III) starting materials in order to realize other structural types for iron phosphonates. A starting material as simple as $FeCl_3\cdot 6H_2O$ produces the desired iron phosphate without the central [$Fe_3(\mu_3$-O)] unit. Upon treatment of two equivalents of *tert*-butylphosphonic acid with a pyridine solution of $FeCl_3\cdot 6H_2O$, the intense red reaction mixture turns immediately yellow. When the stirring was continued at 25 °C for a further 24 h, a light green solution resulted, from which pale-yellow single crystals of $[Fe_{10}(OH)_8(HPO_4)(^tBuPO_3)_8(^tBuPO_3H)_4(py)_8]\cdot 4py\cdot 5H_2O$ (**2**) were isolated after one week (Scheme 1). Because of the poor solubility, compound **2** could not be characterized in solution. The diffuse reflectance UV−visible spectrum shows two intense maxima at 354 and 434 nm, originating from $\pi-\pi^*$ and charge-transfer transitions. The IR spectrum shows characteristic peaks of P═O and M−O−P (ν_{asym} and ν_{sym}) at around 1141, 1072, and 1027 cm^{-1}. The unreacted P−OH groups in the product produce a broad absorption at 2390 cm^{-1}.[3]

Crystal Structure of Decanuclear Phosphonate 2. Compound **2** crystallizes in the tetragonal $I\bar{4}$ space group, and the molecule has a crystallographically imposed −4 symmetry (Figure 3). The complex consists of 10 iron(III) centers, one phosphate anion,[11] eight doubly deprotonated phosphonates, four singly deprotonated phosphonates, eight bridging hydroxide groups, and eight pyridine ligands. A closer look at the complex architecture reveals that the central phosphate anion is responsible for holding the Fe_{10} complex together by forming two major macrocycles, each consisting of five Fe(III) ions and four hydroxide ligands, besides the phosphate anion (Figure 4). The 12-membered $Fe_5(\mu$-

(10) Coxall, R. A.; Harris, S. G.; Henderson, D. K.; Parsons, S.; Tasker, P. A.; Winpenny, R. E. P. *J. Chem. Soc., Dalton Trans.* **2000**, 2349.

(11) If this phosphate anion exists as PO_4^{3-}, then the whole complex will be negatively charged, necessitating the presence of a counter cation in the form of an additional proton. The conductivity studies in the solid state however confirmed the neutral nature of the complex. Hence, a $(HPO_4)^{2-}$ formulation is assumed where the proton is delocalized over the entire unit (all four oxygen atoms are equidistant from P4).

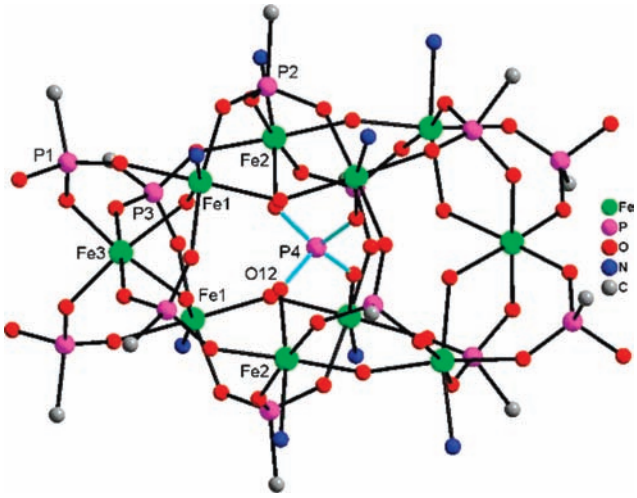

Figure 3. The structure of the core in **2**. Selected bond lengths and bond angles: Fe(1)−O(9)#1 1.954(4), Fe(1)−O(5)#2 1.964(4), Fe(1)−O(11) 1.996(4), Fe(1)−O(1) 2.001(4), Fe(1)−O(10) 2.088(4), Fe(1)−N(1) 2.191(5), Fe(2)−O(12) 1.967(3), Fe(2)−O(7) 1.985(4), Fe(2)−O(11) 1.990(4), Fe(2)−O(6) 1.996(3), Fe(2)−O(4) 2.021(4), Fe(3)−O(8) 1.950(3), Fe(3)−O(8)#3 1.950(3), Fe(3)−O(3)#2 2.006(4), Fe(3)−O(10)#1 2.141(4), Fe(3)−O(10)#2, O(9)#1−Fe(1)−O(5)#2 169.72(16), O(9)#1−Fe(1)−O(11) 82.39(15), O(5)#2−Fe(1)−O(11) 87.52(15), O(9)#1−Fe(1)−O(1) 95.02(16), O(5)#2−Fe(1)−O(1) 94.79(16), O(11)−Fe(1)−O(1) 173.17(16), O(9)#1−Fe(1)−O(10) 92.72(15), O(5)#2−Fe(1)−O(10) 90.91(15), O(11)−Fe(1)−O(10) 99.67(15), O(1)−Fe(1)−O(10) 6.73(16), O(9)#1−Fe(1)−N(1) 88.72(17), O(5)#2−Fe(1)−N(1) 89.67(16), O(11)−Fe(1)−N(1) 92.05(17). Symmetry: (#1) $y-1, -x+1, -z+1$; (#2) $-x, -y+2, z$; (#3) $-y+1, x+1, -z+1$.

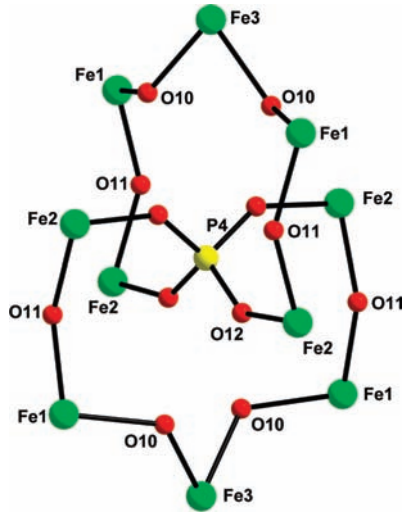

Figure 4. Two $Fe_5(\mu\text{-}OH)_4$ chains joined together by a PO_4 group to form two connected "ferric wheels" around the central phosphorus. The mean planes of the 12-membered rings are orthogonal to each other.

$OH)_4(PO_2)$ rings are nearly planar. These two planes lie orthogonal to each other (due to imposed −4 symmetry) and intersect at the phosphate P4. Thus, the two 12-membered rings can be viewed as molecular ferric wheels which are connected at a common point. The central PO_4 unit (P4), lying on a −4 axis, binds four Fe(III) centers in a [4.1111] fashion with no chelate mode of coordination.

The 10 iron centers are further supported by eight μ_3-O_3P^tBu ligands exhibiting a [3.111] coordination mode and four more μ_2-HO_3P^tBu ligands which exhibit a [2.110] coordination mode. While the [3.111] phosphonates (P2 and P3) bridge the Fe(III) ions from both the rings simultaneously, the [2.110] phosphonate ligands (P1) are found in the periphery of the complex and bridge two adjacent atoms as shown in Figure 3. There are three different types of octahedral iron centers (e.g., Fe1, Fe2, and Fe3) in the structure which differ from each other by their coordination environment. In Fe1, the octahedral sphere is completed by three phosphonate oxygen atoms, two μ-OH, and one pyridine, while the Fe2 ions are surrounded by three phosphonate oxygen atoms, one μ-OH, one pyridine, and the central phosphate ligand. The Fe3 ions, which lie on the −4 axis, have an all-oxygen coordination, being surrounded by four phosphonate oxygen atoms and two μ-OH ligands. The free P−OH groups on P1 present on the periphery of the complex are involved in extensive hydrogen bonding with the lattice water molecules and hence result in the formation of a 1-D polymeric chain of complex **2**, as depicted in Figure 5.

Compound **2** has a unique structure and is the only example of a decanuclear iron cage complex containing a bridging phosphate ligand. Another exclusive structural feature of compound **2** is the absence of μ_3-oxo-centered trimeric iron unit $[Fe_3(\mu_3\text{-}O)]^{7+}$, which is abundant in the case of earlier reported iron phosphonate cage complexes.[6] A few decanuclear iron(III) complexes have been reported so far, and the most interesting among them is a series of decameric iron(III) complexes, $[Fe(OMe)_2(RCOO)]_{10}$, having a cyclic wheel shape.[12] Two iron decanuclear cages $[Fe_{10}O_4(OH)_2(HL)_2(O_2CCMe_3)_{12}(H_2O)_2]\cdot 2H_2O\cdot 5MeCN$ and $[NaFe_{10}O_3(OH)_4(HL)_2(O_2CCMe_3)_{13}]\cdot 2CH_2Cl_2\cdot H_2O$ (HL = 2-[bis(2-hydroxyethyl)amino]-2-(hydroxymethyl)propane-1,3-diol), with stacked butterfly-like core structure have been reported.[13]

The stand-out structural feature of compound **2**, however, is the presence of the central phosphate anion, which has been generated via an in situ hydrolytic cleavage of the P−C bond of $^tBuPO_3H_2$ under very mild reaction conditions employed for the preparation of **2**. The implications of this unintended outcome of the present study are of importance since organophosphonates are used as pesticides and chemical warfare agents, and their irreversible decomposition is of enormous significance for health and environment safety reasons. The phosphorus−carbon bond in organophosphonates is chemically inert, and only some metal oxides are known to irreversibly cleave the P−C bond at higher temperatures in a heterogeneous reaction.[14] To the best of our knowledge, the present synthesis of decanuclear Fe(III)−phosphate−phosphonate **2** provides the first example of room-temperature P−C bond cleavage in a homogeneous medium. While $FeCl_3$ seems to catalyze this cleavage in the presence of pyridine, the trimeric Fe(III) precursor complex under identical conditions does not produce such a conver-

(12) (a) Taft, K. L.; Lippard, S. J. *J. Am. Chem. Soc.* **1990**, *112*, 9629. (b) Jiang, G.; Li, Y.; Hua, W.; Song, Y.; Bai, J.; Li, S.; Scheer, M.; You, X. *Cryst. Eng. Commun.* **2006**, *8*, 384. (c) Taft, K. L.; Delfs, C. D.; Papaefthymiou, G. C.; Foner, S.; Gatteschi, D.; Lippard, S. J. *J. Am. Chem. Soc.* **1994**, *114*, 823.
(13) Ferguson, A.; McGregor, J.; Parkin, A.; Murrie, M. *Dalton Trans.* **2008**, 731.
(14) Ekerdt, J. G.; Klabunde, K. J.; Shapley, J. R.; White, J. M.; Yates, J. T., Jr. *J. Phys. Chem.* **1988**, *92*, 6182.

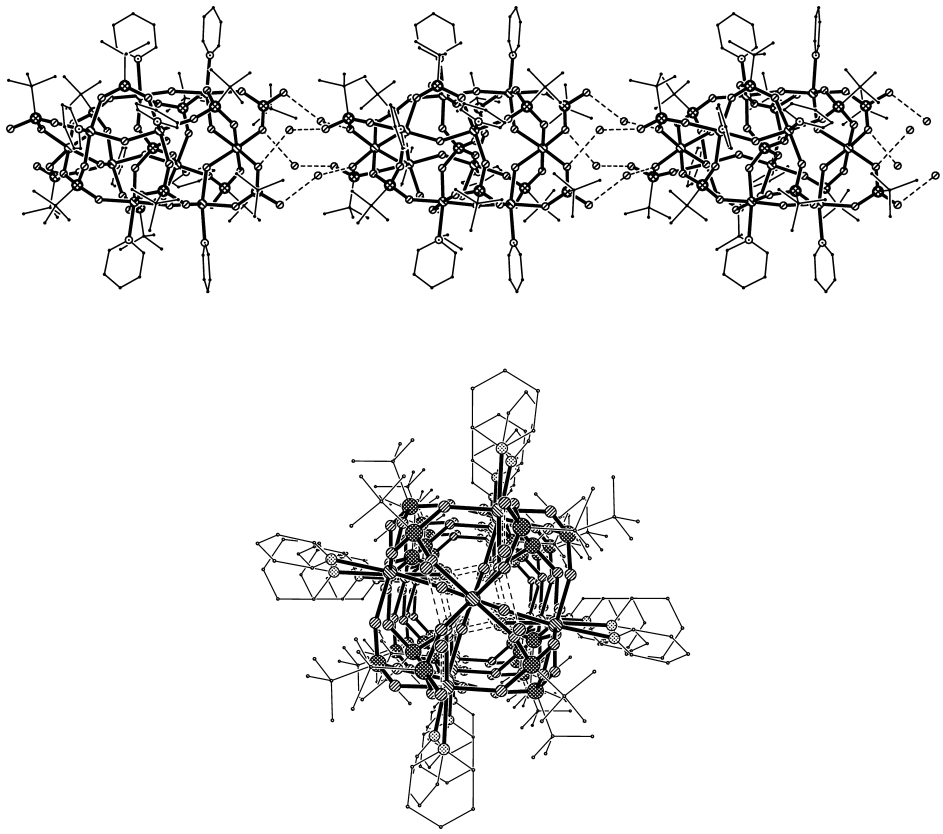

Figure 5. Water-bridged polymeric chain of **2** viewed along the *b* axis (above) and *c* axis (below).

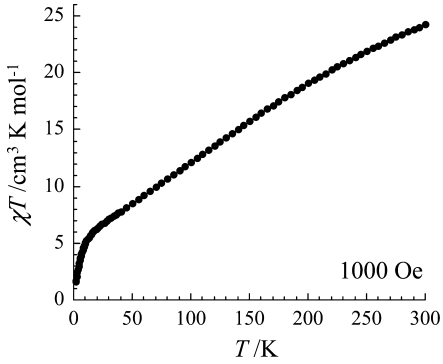

Figure 6. Temperature dependence of the magnetic susceptibility for **2** at 1000 Oe.

sion during the synthesis of **1**. To prove this premise, the reaction mixture leading to the formation of **2** was subjected to a gas chromatographic analysis. The reaction mixture indeed exhibited a very weak band for ^{t}BuOH (formed in the course of the reaction through the hydrolysis of ^{t}BuPO$_3$H$_2$; see the Supporting Information). Thus, the use of other Fe(III) salts under similar reaction conditions not only would unravel other potential promoters of the cleavage reactions but also would shed some light on the possible mechanism of the cleavage reaction.

Magnetic Properties of 2. The presence of cage architectures in **1** and **2** with varying Fe···Fe separations is expected to lead to interesting magnetic exchange between the metal ions. Since the structure of **1** is similar to the earlier reported tetrameric Fe(III)−phosphonates[6a−c] (cf. Table 1 for a structural comparison), temperature-dependent magnetic studies were not performed. However, due to the uniqueness of structure of **2**, its magnetic behavior was studied in detail. As already seen in related Fe(III) systems,[6c,d,7] the temperature dependence of the χT product (shown in Figure 6) reveals dominant antiferromagnetic interactions between Fe(III) centers in **2**. This result is supported by the room-temperature χT product, which is much lower (24.4 cm^3 K mol^{-1}) than expected for 10 isolated $S = 5/2$ Fe(III) spins (43.75 cm^3 K mol^{-1} with $g = 2$), and by the gradual decrease of χT from 300 to 1.8 K (1.6 cm^3 K mol^{-1}). On the basis of the χT versus T data between 10 and 1.8 K, the absence of a plateau in this temperature domain, and the extrapolation of χT below 1.8 K, the ground state of this complex is very likely $S = 0$.

Conclusions

We have shown that the use of a triangular complex as a precursor for the preparation of Fe(III) phosphonates results in the formation of tetranuclear complex **1**, which still retains the [Fe$_3$(μ_3-O)] central core, as has also been the case with the majority of the earlier studies in the literature. The use of FeCl$_3$·6H$_2$O as the iron source and pyridine as the solvent, to the contrary, yields the novel decanuclear complex **2** with an unprecedented architecture. In the process of the synthesis of **2**, it has also been possible to demonstrate the previously unknown P−C bond cleavage of a phosphonic acid in a homogeneous medium at room temperature, which has been supported by the GC analysis of the reaction mixture.[15] It appears that it would be possible to extend this work to

(15) The presently available information however is insufficient to postulate a mechanism for the observed P−C cleavage reaction.

realize other types of Fe−phosphate−phosphonate complexes by also enhancing the extent of P−C cleavage. We are currently investigating these aspects.

Experimental Section

Materials and Methods. Starting materials were procured from commercial sources and used as received. Solvents were purified by conventional techniques and distilled prior to use. Elemental analyses were performed on a Carlo Eraba (Italy) Model 1106 Elemental Analyzer. The melting points were measured in glass capillaries and were reported uncorrected. Infrared spectra were recorded on a Perkin-Elmer FT-IR spectrometer as KBr diluted discs. UV−visible spectra were obtained on a Shimdzu UV-260 spectrophotometer. Gas chromatographic analyses were performed on a Shimadzu-15A Gas Chromatograph.

Synthesis of $[Fe_4O(^tBuPO_3)_3(O_2CPh)_3(Py)_3Cl]\cdot 3.5py$ (1). To a continuously stirred dark brown solution of $[Fe_3O(O_2CPh)_6(H_2O)_3]Cl$[16] (0.499 g, 0.5 mmol) in pyridine (25 mL) was added solid $^tBuPO_3H_2$ (0.138 g, 1 mmol) at room temperature. As stirring was continued for 24 h, the color of the reaction mixture turned to bright yellow, after which it was filtered. Diffusion of petroleum ether to the filtrate at ambient temperature produced dark yellow crystals of **1** after three days. Yield: 0.076 g (12% based on Fe). Mp > 250 °C. Elem anal. (%) calcd for **1** ($C_{68}H_{77}ClFe_4N_7O_{16}P_3$): C, 51.04; H, 4.85; N, 6.13. Found: C, 53.01; H, 4.81; N, 5.89. DRUV−vis (nm): 415, 493. IR (ν/cm^{-1}, KBr pellets): 3430(br), 3064(w), 2970(m), 2945(m), 2859(w), 1602(s), 1562(vs), 1477(w), 1447(m), 1417(s), 1218(w), 1131(vs), 1084(s), 1070(s), 1005(vs), 841(w), 758(w), 719(m), 699(m), 594(w), 505(m).

Synthesis of $[Fe_{10}(OH)_8(HPO_4)(^tBuPO_3)_8(^tBuPO_3H)_4(py)_8]\cdot 4py\cdot 5H_2O$ (2). $FeCl_3\cdot 6H_2O$ (0.270 g, 1 mmol) was dissolved in 30 mL of pyridine to obtain an intense red solution. To this was added solid $^tBuPO_3H_2$ (0.276 g, 2 mmol), and the resultant mixture was stirred for 24 h at ambient temperature, during which the color of the reaction mixture turned light green. The resulting light green solution was filtered, and the filtrate was left undisturbed at room temperature to obtain block-shaped light yellow crystals after one week. Yield: 0.052 g (15% based on iron). Mp > 250 °C. Elem anal. (%) calcd for **2** ($C_{108}H_{191}Fe_{10}N_{12}O_{53}P_{13}$): C, 37.41; H, 5.55; N, 4.84. Found: C, 38.04; H, 5.40; N, 4.30. DRUV−vis (nm): 354, 434. IR (ν/cm^{-1}, KBr pellets): 3450(br), 2951(m), 2867(w), 2390(br), 1635(w), 1605(m), 1539(w), 1477(m), 1448(m), 1390(w), 1201(w), 1141(s), 1072(s), 1027(vs), 923(m), 832(w), 756(w), 756(w), 705(m), 656(s), 511(s).

X-Ray Diffraction Studies. Suitable single crystals of compounds **1** and **2**, obtained directly from the reaction mixtures, were used for diffraction measurements. The diffraction data for both compounds were obtained on an Oxford Diffraction XCalibur-S CCD system operating at 150 K. The structure solution and refinement were carried out using the SIR-92 and SHELXL-96 programs, respectively.[17] All non-hydrogen atoms were subjected to anisotropic refinement. The hydrogen atoms were placed on calculated positions but were allowed to ride on their parent atoms during subsequent cycles of refinement.

Crystal data for **1**: $C_{65.5}H_{74.5}ClFe_4N_{6.5}O_{16}P_3$, M = 1560.58 g mol^{-1}, monoclinic, $P2_1/n$, Z = 4, a = 14.7362(4) Å, b = 25.4076(6) Å, c = 20.3945(5) Å, β = 91.594(2)°, V = 7633.0(3) Å^3, T = 150(2) K, λ = 0.71073 Å, D_{calcd} = 1.358 g cm^{-3}, μ(Mo Kα) = 0.907 mm^{-1}, F(000) = 3228, θ range = 3.02−25.00 °, reflections = 68 075, parameters = 826, crystal size = 0.32 × 0.25 × 0.22 mm^3, R_1 ($I > 2\sigma(I)$) = 0.0982, wR_2 = 0.2330, GOF = 1.051.

Crystal data for **2**: $C_{108}H_{191}Fe_{10}N_{12}O_{53}P_{13}$, M = 3466.84 g mol^{-1}, tetragonal, $I\bar{4}$, Z = 2, a = 20.9311(4) Å, b = 20.9311(4) Å, c = 17.3409(6) Å, V = 7597.2(3) Å^3, T = 150(2) K, λ = 0.71073 Å, D_{calcd} = 1.516 g cm^{-3}, μ(Mo Kα) = 1.146 mm^{-1}, F(000) = 3604, θ range = 3.08−24.99 °, reflections = 24 979, parameters = 406, crystal size = 0.22 × 0.17 × 0.11 mm^3, R_1 ($I > 2\sigma(I)$) = 0.0433, wR_2 = 0.0927, GOF = 0.938.

Magnetic Measurements. The magnetic susceptibility measurements were obtained with the use of a Quantum Design SQUID magnetometer MPMS-XL. This magnetometer works between 1.8 and 400 K for dc applied fields ranging from −7 to +7 T. Measurements were performed on a polycrystalline sample of 21.70 mg. Even if no hysteresis on the M versus H data has been observed above 1.8 K, the ac susceptibility of this compound has been measured in a zero dc field with an oscillating ac field of 3 Oe and ac frequencies ranging from 1 to 1500 Hz. Above 1.8 K, the ac susceptibility does not have an out-of-phase component; that is, this compound does not show features expected when slow relaxation of the magnetization is observed like in single-molecule magnets. The magnetic data were corrected for the sample holder and the diamagnetic contribution.

Acknowledgment. This work was supported by DST, New Delhi. N.G. thanks CSIR, New Delhi for a research fellowship. We thank the DST-funded National Single Crystal Diffraction Facility at IIT-Bombay for the diffraction data and SAIF, IIT-Bombay for the spectral data. We also thank the European network MAGMANet (NMP3-CT-2005-515767), the University of Bordeaux, the CNRS and the Région Aquitaine for financial supports.

Supporting Information Available: Details of X-ray structure investigations (CIF). This material is available free of charge via the Internet at http://pubs.acs.org.

IC8017562

(16) (a) Blake, A. B.; Fraser, L. R. *J. Chem. Soc., Dalton Trans.* **1975**, 193. (b) Johnson, M. K.; Powell, D. B.; Cannon, R. D. *Spectrochim. Acta, Part A* **1981**, *37*, 995.

(17) (a) Altomare, A.; Cascarano, G.; Giacovazzo, C.; Gualardi, Z. *J. Appl. Crystallogr.* **1993**, *26*, 343. (b) Sheldrick, G. M. *SHELXL-97*; University of Göttingen: Göttingen, Germany, 1997.